

Magnetoelectric effect in $R_2\text{CuO}_4$ ($R = \text{Gd}, \text{Sm}, \text{and Nd}$)

H. Wiegelmann

*Grenoble High Magnetic Field Laboratory, Max-Planck-Institut für Festkörperforschung
and Centre National de la Recherche Scientifique, Boîte Postale 166, F-38042 Grenoble Cedex 9, France*

I. M. Vitebsky

*Grenoble High Magnetic Field Laboratory, Max-Planck-Institut für Festkörperforschung
and Centre National de la Recherche Scientifique, Boîte Postale 166, F-38042 Grenoble Cedex 9, France
and Sage Technology Inc., Smyrna, Georgia 30080*

A. A. Stepanov

*Grenoble High Magnetic Field Laboratory, Max-Planck-Institut für Festkörperforschung
and Centre National de la Recherche Scientifique, Boîte Postale 166, F-38042 Grenoble Cedex 9, France
and B. Verkin Institute for Low Temperature Physics and Engineering, Ukrainian Academy of Sciences, 310164 Kharkov, Ukraine*

A. G. M. Jansen and P. Wyder

*Grenoble High Magnetic Field Laboratory, Max-Planck-Institut für Festkörperforschung
and Centre National de la Recherche Scientifique, Boîte Postale 166, F-38042 Grenoble Cedex 9, France*

(Received 10 October 1996; revised manuscript received 18 February 1997)

In strong magnetic fields up to 20 T the magnetoelectric (ME) effect has been measured in the tetragonal antiferromagnets $R_2\text{CuO}_4$, $R = \text{Gd}, \text{Sm}, \text{and Nd}$, which are parent compounds for high- T_c superconductivity. For the Gd_2CuO_4 and Sm_2CuO_4 compounds a symmetry analysis yields that the ME effect is associated with the antiferromagnetically ordered rare-earth subsystem. From the magnetic field and temperature dependence of the ME effect in Gd_2CuO_4 some very detailed conclusions can be drawn about the nature of the magnetic ordering which appear to be in agreement with the magnetic structure revealed in this compound. For Sm_2CuO_4 in addition to the ME effect a distinct ferroelectric behavior has been observed which is only compatible with a lower crystal symmetry than it has been thought to be. It raises the question of whether superconductivity in Ce-doped Sm_2CuO_4 coexists with ferroelectricity. The ME-effect data in high magnetic fields show evidence for magnetic phase transitions, associated with a rearrangement of the intrinsic rare-earth magnetic structure. From the obtained (H, T) phase diagrams of Gd_2CuO_4 and Sm_2CuO_4 critical exponents [$\beta(\text{Gd}) \approx 0.4$ and $\beta(\text{Sm}) \approx 0.5$] were found and it can be concluded that the intrinsic ordering of the rare-earth magnetic subsystem is of three-dimensional character. In the case of Nd_2CuO_4 , the adopted crystal and magnetic structure of this compound rules out any kind of ME effect. Nevertheless, we have observed some weak but distinct ME response, which suggests the existence of a spontaneous structural distortion within the CuO_2 planes. [S0163-1829(97)02022-5]

I. INTRODUCTION

Recently a new class of copper-oxide superconductors $R_{2-x}\text{Ce}_x\text{CuO}_4$ ($R = \text{Pr}, \text{Nd}, \text{Sm}, \text{and Eu}$) has been discovered^{1,2} and has become the subject of an intense study due to a variety of uncommon properties. First of all $R_{2-x}\text{Ce}_x\text{CuO}_4$ compounds exhibit electron-type conductivity in contrast to the related $\text{La}_{2-x}\text{M}_x\text{CuO}_4$ ($M = \text{Ca}, \text{Sr}, \text{Ba}, \text{or Na}$) compounds showing hole-type conductivity.³ Second, unlike in $R\text{BaCuO}$ compounds where the substitution of trivalent rare-earth ions had little effect on their superconductivity, in electron-doped $R_{2-x}\text{Ce}_x\text{CuO}_4$ compounds the rare-earth subsystem affects strongly both magnetic and superconducting properties. According to Ref. 4 the superconductivity of $R_{2-x}\text{Ce}_x\text{CuO}_4$ is observed only for compounds containing the light rare-earth ions (Pr, Nd, Sm, and Eu), and no superconductivity is observed in compounds with heavier rare-earth ions, starting from Gd.

Magnetic ordering of the Cu magnetic moments has been

found in all parent compounds $R_2\text{CuO}_4$ with a Néel temperature $T_N(\text{Cu})$ just below room temperature.⁵ The corresponding magnetic structure is of two-dimensional character. In the temperature range of several kelvin a magnetic ordering of the rare-earth magnetic moments has been observed for $R = \text{Gd}, \text{Sm}, \text{Nd}, \text{and Pr}$, whereas no ordering has been found for Eu. The magnetic subsystems have been studied by neutron diffraction, specific heat, and various other experimental techniques, and substantial differences in the magnetic ordering have been found in each compound.

In this context, Gd_2CuO_4 and Sm_2CuO_4 occupy a unique place in this class of materials. In both compounds a symmetry-breaking magnetic ordering of the rare-earth subsystem has been observed in contrast to other members of this class. Considering the possible correlation between “nonsuperconducting” and magnetic properties of Gd_2CuO_4 and the coexistence of rare-earth magnetic ordering and superconductivity in Sm_2CuO_4 and Nd_2CuO_4 , it is of main concern to study the magnetic properties in order to

elucidate the role of the rare-earth ions in forming the electronic properties of $R_{2-x}\text{Ce}_x\text{CuO}_4$ and of the parent compound $R_2\text{CuO}_4$.

The linear and nonlinear magnetoelectric (ME) effect is extremely sensitive to the specific magnetic and crystal symmetry of a system. The knowledge of the actual character of the effect in combination with a symmetry-based theoretical analysis can bring a lot of valuable information about the crystal and magnetic structure of a system. This could be especially important for small symmetry-violating distortions of crystal and spin structures. Whether or not a certain component of a magnetoelectric tensor is zero is an inherent property of a crystal that cannot be affected by any sort of randomly distributed defects. To put it differently, a magnetoelectric effect can clearly distinguish a symmetry-lowering coherent distortion of the crystal, however small they are, but crystal imperfections do not substantially influence the magnetoelectric effect of a crystal. So the results obtained by magnetoelectric measurements remain reliable even in the case of very imperfect crystals. The study of magnetoelectricity can be very helpful for the determination of the actual crystal and spin structure of high-temperature superconductors, all of which being based on antiferromagnetically ordered oxides with rather unstable crystal structures.

In this paper we would like to review the experimental results on the ME effect in $R_2\text{CuO}_4$, $R=\text{Gd}, \text{Sm},$ and Nd . Preliminary results have already been reported for Gd_2CuO_4 .^{6,7} By comparing the experimental results for the isostructural compounds Gd_2CuO_4 and Sm_2CuO_4 , subtle differences in the magnetic ordering are clearly resolved, and by extending the investigation to higher magnetic fields at several temperatures, information about magnetic phase transitions is added. Finally, using ME measurements we have revealed that the actual crystal structures of Sm_2CuO_4 and Nd_2CuO_4 are different from what they were thought to be. Specifically, in this class of compounds, a spontaneous electric polarization has been found in Sm_2CuO_4 , which suggests a lower crystal symmetry than $I4/mmm$. A similar conclusion regarding the crystal symmetry of Nd_2CuO_4 can be drawn from the observation of the ME effect in this compound. Unlike Gd_2CuO_4 and Sm_2CuO_4 , it is the copper magnetic subsystem that is responsible for a nonzero ME response in Nd_2CuO_4 . This is why the magnitude of the effect in this latter case proves to be much smaller.

II. MAGNETIC PROPERTIES

Apart from some possible small distortions, the crystal structure of all representatives of the $R_2\text{CuO}_4$ family ($R=\text{Pr}, \text{Nd}, \text{Sm}, \text{Eu},$ and Gd) belongs to the T' phase of the tetragonal body-centered lattice with space symmetry of $I4/mmm$. It can be represented as a stack of copper-oxygen layers sandwiched between double layers each containing either a rare earth or oxygen ion.

The copper subsystem of $R_2\text{CuO}_4$ orders antiferromagnetically in the temperature range of $270 \text{ K} < T_N < 290 \text{ K}$. The dominant spin-spin interaction for all compounds is the isotropic exchange coupling between neighboring copper ions within a CuO_2 plane given by the spin Hamiltonian

$$\mathcal{H}_{\text{ex}}(n) = J \sum_i \mathbf{S}_i(n) \mathbf{S}_{i+1}(n), \quad (1)$$

where $J > 0$ and n is any of the CuO_2 planes.

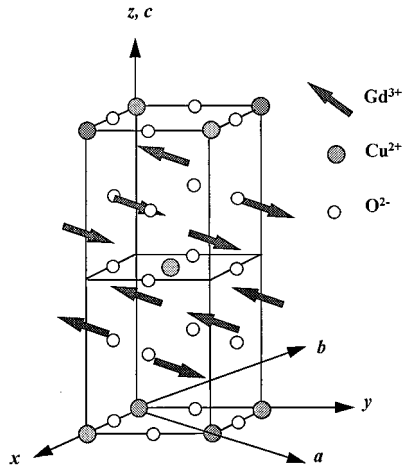
The ground state of the copper spin system is the quasi-two-dimensional ‘‘chessboard’’ antiferromagnetic ordering with a propagation vector $\kappa = (\frac{1}{2}, \frac{1}{2}, 0)$; the spins lie in the CuO_2 plane, forming an ‘‘easy-plane’’ antiferromagnet as it is imposed by the intraplane anisotropy. This is a typical spin arrangement for tetragonal body-centered crystals.

The ‘‘chessboard’’-like ordering leads to a doubling of the magnetic unit cell and the emergence of an antitranslation operation $T'_a \equiv 1' \times T_a^-$ in the magnetic space group of the crystal. As a result, both time and space inversion operations enter the magnetic point group, and the crystal belongs to the nonmagnetic class. No magnetoelectric effect can exist in such a system.

One peculiarity of the Cu magnetic subsystem in Gd_2CuO_4 was the observation of weak ferromagnetism in the temperature range of $20 \text{ K} < T < T_N(\text{Cu}) = 285 \text{ K}$ which has not been found in any other rare-earth cuprates of this family.^{2,4,5,8,9} The existence of weak ferromagnetism is incompatible with the crystal symmetry $I4/mmm$ of the system. Precise x-ray and neutron diffraction experiments have nevertheless shown no sign of a violation of the tetragonal symmetry. To resolve this contradiction a picture has been put forward in which a certain structural distortion occurs within each CuO_2 plane but being uncorrelated from plane to plane¹⁰.

A. R subsystem

While the copper moments are antiferromagnetically ordered just below the room temperature, the rare-earth subsystem remains paramagnetic down to temperatures of a few kelvin. An inherent long-range antiferromagnetic order with the propagation vector $\kappa = (0, 0, 0)$ emerges at $T_N(\text{Gd}) = 6.5 \text{ K}$ for Gd_2CuO_4 and at $T_N(\text{Sm}) = 5.9 \text{ K}$ for Sm_2CuO_4 . In these two compounds a rare-earth ordering temperature $T_N(R)$ is clearly observable by a sharp peak in the specific heat.^{11,12} The specific spin arrangements are known from neutron diffraction experiments.¹³ For the Gd subsystem the neutron experiments show that in the intermediate temperature range $T_N(R) < T < T_N(\text{Cu})$ the rare-earth moments are magnetically polarized by the ordered copper subsystem. Below $T_N(\text{Gd}) = 6.5 \text{ K}$ the rare-earth magnetic subsystem of Gd_2CuO_4 consists of ferromagnetic Gd planes, parallel to the CuO_2 planes, with neighboring planes antiferromagnetically coupled. In contrast to the copper subsystem, the intrinsic rare-earth spin arrangement removes the space inversion but does not affect the translation symmetry. As a consequence, the two magnetic subsystems below $T_N(\text{Gd})$ manifest themselves rather independently both in static and resonance experiments. Antiferromagnetic resonance and magnetic measurements made below $T_N(\text{Gd})$ also indicate that Gd_2CuO_4 is an ‘‘easy-plane’’ antiferromagnet¹³ with the Gd spins aligned along the $[110]$ direction in zero magnetic field. Under applied magnetic field, a continuous spin reorientation at $H = 0.88 \text{ T}$ ($T = 1.8 \text{ K}$) and a spin-flip transition at $H_{\text{sf}} = 11 \text{ T}$ ($T = 1.5 \text{ K}$) have been observed.

FIG. 1. Proposed magnetic structure for Gd_2CuO_4 (Ref. 13).

Knowing the actual magnetic structure of Gd_2CuO_4 represented in Fig. 1 below $T_N(\text{Gd})$, one can state that the magnetic symmetry of this compound belongs to the orthorhombic magnetic class $mm'm$ which allows a linear ME effect with two independent nonzero components of the ME tensor

$$\alpha_{ij} = \begin{pmatrix} 0 & 0 & \alpha_{ac} \\ 0 & 0 & 0 \\ \alpha_{ca} & 0 & 0 \end{pmatrix}, \quad (2)$$

where α is defined in the usual way:

$$\alpha_{ij} = \frac{\partial P_i}{\partial H_j}, \quad (3)$$

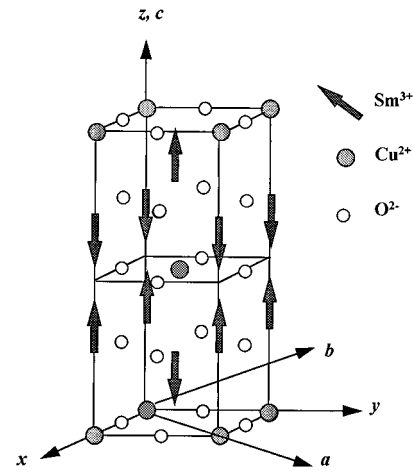
\mathbf{P} being the electric polarization in an applied magnetic field \mathbf{H} . The indices i, j refer to the orthorhombic axes $\mathbf{a} \parallel [1, 1, 0]$, $\mathbf{b} \parallel [1, -1, 0]$, $\mathbf{c} \parallel [0, 0, 1]$, imposed upon the tetragonal crystal structure by the antiferromagnetic spin arrangement. Above $T_N(\text{Gd})$ the crystal symmetry is incompatible with a nonzero electric polarization even in the presence of an external magnetic field because of the space inversion operation.

As in the case of Gd_2CuO_4 , in Sm_2CuO_4 below $T_N(\text{Sm})$ the rare-earth spin structure consists of ferromagnetic sheets, the neighboring layers being antiferromagnetically coupled. But this time the rare-earth spins are oriented along the $[001]$ direction as shown in Fig. 2.¹⁵ The corresponding magnetic symmetry belongs to the orthorhombic magnetic class $m'm'm'$ which allows a linear magnetoelectric effect with three independent nonzero components of the ME tensor

$$\alpha_{ij} = \begin{pmatrix} \alpha_{aa} & 0 & 0 \\ 0 & \alpha_{bb} & 0 \\ 0 & 0 & \alpha_{cc} \end{pmatrix}. \quad (4)$$

Again, above $T_N(\text{Sm})$ the magnetic symmetry based on the assumed crystal and magnetic structure is incompatible with ME effect.

At this point the usefulness of the ME effect in determining the magnetic ground state should be emphasized. Gd_2CuO_4 and Sm_2CuO_4 possess rather similar magnetic

FIG. 2. Proposed magnetic structure for Sm_2CuO_4 (Ref. 15).

structures, except for the direction of the rare-earth spins in the ferromagnetic layers. The latter circumstance suffices to change the form of the ME susceptibility tensor α completely and the magnetic ground state can be distinguished by measuring any of the ME tensor components.

The relatively high rare-earth ordering temperatures in Gd_2CuO_4 and Sm_2CuO_4 suggest that the dominant interaction between the rare-earth spins is of exchange origin through the CuO_2 layers. Indeed, taking into account the difference between magnetic moments of the trivalent rare-earth ions [Gd^{3+} : $\mu = 6.5\mu_B$ (Ref. 13); Sm^{3+} : $\mu = 0.37\mu_B$ (Ref. 15)] one can conclude that the Sm ordering temperature would be much lower if the interaction responsible for the intrinsic rare-earth antiferromagnetic order were primarily of dipole-dipole origin. Thus, the ordering of the Sm spins should substantially influence the superconducting properties of $\text{Sm}_{1.85}\text{Ce}_{0.15}\text{CuO}_4$, but a direct indication for such an influence has not been obtained.^{15,16}

In the case of Nd_2CuO_4 , the spin-spin coupling between the Cu and Nd sublattices is the only cause for the finite magnetic polarization of the rare-earth ions at arbitrarily low temperatures.¹⁴ The magnitude of the induced magnetic polarization increases continuously with decreasing temperature without a magnetic phase transition. There is no intrinsic antiferromagnetic order within the Nd magnetic subsystem, and the magnetic symmetry of Nd_2CuO_4 is completely determined by the ordered Cu sublattices. If the actual crystal symmetry of Nd_2CuO_4 were precisely described by the space group of $I4/mmm$, the corresponding macroscopic magnetic symmetry would be mmm , that is, of a nonmagnetic kind. A ME effect is forbidden for such a symmetry.

III. PHENOMENOLOGICAL CONSIDERATIONS FOR Gd_2CuO_4 AND Sm_2CuO_4

As has been said before, it is the rare-earth magnetic subsystem which is responsible for the ME effect in Gd_2CuO_4 and Sm_2CuO_4 , and neither the Cu-Cu nor Cu-R spin-spin interaction affects substantially the character of the effect. Hence, when constructing the phenomenological description of the ME effect in Gd_2CuO_4 and Sm_2CuO_4 , one can ignore the copper sublattices.

Since we deal with the ME effect in Gd_2CuO_4 and Sm_2CuO_4 not only in small external magnetic fields, we cannot restrict ourselves to the linear effect described by the tensor α from Eq. (2) or (4). To obtain the induced electric polarization as a function of an arbitrarily strong magnetic field we have to employ a phenomenological model. Following this phenomenological approach the state of the rare-earth magnetic subsystem is specified by two vectors $\mathbf{L}=\mathbf{S}_1-\mathbf{S}_2$ and $\mathbf{M}=\mathbf{S}_1+\mathbf{S}_2$, where \mathbf{S}_1 and \mathbf{S}_2 denote the rare-earth sublattice magnetizations. The entire phenomenological free energy can be represented as a sum of three contributions

$$W(\mathbf{S}, \mathbf{P}) = W_m(\mathbf{S}) + W_{\text{ME}}(\mathbf{S}, \mathbf{P}) + W_e(\mathbf{P}), \quad (5)$$

where $W_m(\mathbf{S})$ is a purely magnetic contribution to the total free energy, $W_{\text{ME}}(\mathbf{S}, \mathbf{P})$ is a ME one, and $W_e(\mathbf{P})$ is a purely electric contribution. All equilibrium properties of a magnetic subsystem including a sought dependence $\mathbf{P}(\mathbf{H})$ can be found by minimizing $W(\mathbf{S}, \mathbf{P})$ with respect to \mathbf{S} and \mathbf{P} .

The first term on the right-hand side of Eq. (5) determines the ground state of the magnetic system and, eventually, whether or not a ME effect will occur. The main contribution to the magnetic energy $W_m(\mathbf{S})$ is given by the expression

$$W_m(\mathbf{S}) = J\mathbf{S}_1\mathbf{S}_2 + f(\mathbf{S}_1^2) + f(\mathbf{S}_2^2) + a_1(S_{1z}^2 + S_{2z}^2) - 2a_2S_{1z}S_{2z} - bL_x^2L_y^2 - \mathbf{M}\mathbf{H}. \quad (6)$$

The first term on the right-hand side describes the antiferromagnetic exchange interaction between the rare-earth sublattices (the neighboring rare-earth planes). The terms $f(\mathbf{S}_1^2)$ and $f(\mathbf{S}_2^2)$ include the intraplane exchange coupling (intrasublattice exchange interaction of ferromagnetic type) as well as the entropy contribution to the free energy. The following three terms in Eq. (6) describe the energy of uniaxial and in-plane magnetic anisotropy; these terms are responsible for the equilibrium orientation of the rare-earth spins relative to the crystallographic axes. The last term is a Zeeman contribution. Among other things, the first three terms in the expression for $W_m(\mathbf{S})$ in a combination with Zeeman energy are responsible for the temperature and field dependence of the sublattice magnetization magnitudes.

Gd_2CuO_4 belongs to the class of low-anisotropy (Heisenberg) antiferromagnets due to the zero orbital moment of the ground state of the Gd^{3+} ions. This situation corresponds to the following interrelation between the different magnetic parameters in Eq. (6): $J \gg a_1$, $a_2 \gg b > 0$. In the absence of a magnetic field the ground state of $W_m(\mathbf{S})$ for $a_1 - 2a_2 > 0$ is described by

$$\mathbf{L} \parallel \mathbf{a} \parallel [110], \quad \mathbf{M} = 0, \quad (7)$$

considering only one of the four orientational domains. An external magnetic field distorts the magnetic structure (7) and, eventually, breaks completely the antiferromagnetic arrangement of the rare-earth spins at $H > H_c$:

$$\mathbf{L} = 0, \quad \mathbf{M} = 2\mathbf{S}. \quad (8)$$

This state is commonly called a paramagnetic one (sometimes, the above high-field state is called a ferromagnetic state, which is equally reasonable if $M \neq 0$). In the case of

Gd_2CuO_4 , H_c coincides with the critical field H_{sf} of the spin-flip phase transition between the phases with $\mathbf{L} \neq 0$ and $\mathbf{L} = 0$.

The zero-field magnetic ground state of Sm_2CuO_4 , which belongs to the class of ‘‘easy-axis’’ antiferromagnets with relatively strong uniaxial anisotropy, is

$$\mathbf{L} \parallel \mathbf{c} \parallel [001], \quad \mathbf{M} = 0, \quad (9)$$

which corresponds to $a_1 - 2a_2 < 0$. If the temperature is much lower than $T_N(R)$, we can put $M^2 + L^2 = 1$, $\mathbf{L}\mathbf{M} = 0$. If, then, the uniaxial anisotropy is stronger than the intersublattice antiferromagnetic exchange interaction J , an external magnetic field parallel to the spin direction leaves the magnetic structure (9) almost unchanged up to the critical field $H_c = J$, where a first-order phase transition to the paramagnetic state occurs. The paramagnetic (or ferromagnetic) state is stable for any $H > H_c$.

In both cases, irrespective of the magnetic field direction the magnetic symmetry group of the paramagnetic phase (8) presumably contains the space inversion $1'$, and no electric polarization has been expected to exist. Obviously, H_c vanishes as $T \rightarrow T_N(R)$.

To find the dependence $\mathbf{P}(\mathbf{H})$ for $H < H_c$ one should consider the remaining two contributions to $W(\mathbf{S}, \mathbf{P})$ in Eq. (5). Taking into account the specific symmetry of the system one can easily obtain the following expression for the ME contribution:

$$W_{\text{ME}}(\mathbf{S}, \mathbf{P}) = \Lambda P_z \mathbf{M}\mathbf{L} + \lambda_z P_z M_z L_z + \lambda_1 (L_z M_x P_x + L_z M_y P_y) + \lambda (M_z L_x P_x + M_z L_y P_y). \quad (10)$$

The first term on the right is of an exchange nature and the corresponding contribution to the ME effect is associated with the violation of the equality of the sublattice magnetization magnitudes. The remaining terms on the right-hand side of Eq. (10) are of relativistic origin; i.e., they result from the relativistic part of the spin-spin and spin-lattice coupling.

To complete the construction of the free energy (5) we write down the electric contribution:

$$W_e(\mathbf{P}) = \frac{1}{2\kappa_{zz}} P_z^2 + \frac{1}{2\kappa_{xx}} (P_x^2 + P_y^2) - \mathbf{E}\mathbf{P}, \quad (11)$$

where κ denotes the components of the electric susceptibility of the system.

To calculate electric polarization \mathbf{P} as a function of an applied magnetic field \mathbf{H} we have to minimize $W(\mathbf{S}, \mathbf{P})$ with respect to sublattice magnetizations and electric polarization under a fixed external field. In the case of a small external magnetic field the results boil down to some explicit expressions for the different components of the tensor α for the linear ME effect in terms of the phenomenological coefficients in the expression for $W(\mathbf{S}, \mathbf{P})$.

In the case of Gd_2CuO_4 , only the first and the last terms on the right-hand side of Eq. (10) contribute to the linear ME effect; specifically,

$$\alpha_{ca} = \frac{\partial P_c}{\partial H_a} = 2S\Lambda\chi_{\parallel}\kappa_{zz}, \quad (12)$$

$$\alpha_{ac} = \frac{\partial P_a}{\partial H_c} = S\lambda\chi_{\perp}\kappa_{xx}, \quad (13)$$

where

$$\chi_{\parallel} = 2Sf''(S^2) \quad \text{and} \quad \chi_{\perp} = J^{-1} \quad (14)$$

denote the magnetic susceptibilities along and perpendicular to the vector \mathbf{L} , respectively. Obviously, the longitudinal susceptibility χ_{\parallel} decreases sharply as the temperature tends to zero. The two nonzero components α_{ca} and α_{ac} have an exchange and a relativistic origin, respectively.

For Sm_2CuO_4 only the first three terms on the right-hand side of Eq. (10) contribute to the nonzero components of the tensor α in Eq. (4). The corresponding expressions are obtained in analogy to Eqs. (12) and (13).

IV. EXPERIMENTAL DETAILS

The single crystals of Gd_2CuO_4 , Sm_2CuO_4 , and Nd_2CuO_4 used in these experiments were grown by the flux method using CuO as flux material.¹⁷ The edges of the sample coincided with the tetragonal axes at room temperature and were of the dimensions $(5.00 \times 1.41 \times 0.75) \text{ mm}^3$ for Gd_2CuO_4 , $(3.19 \times 2.03 \times 0.84) \text{ mm}^3$ for Sm_2CuO_4 , and $(15.9 \times 2.10 \times 0.94) \text{ mm}^3$ for Nd_2CuO_4 . Electrodes were deposited by silver paint on the appropriated faces and the contacted samples were fixed to the sample holder by varnish. In a liquid helium cryostat the temperature was varied between 1.3 K and 15 K and measured by a calibrated RuO thermometer.

The measurements were performed in static magnetic fields up to 20 T using a dc measuring technique, where the current between electrodes was measured and integrated, leaving the sample at zero electric field. The integrated value was scaled and displayed as an electric charge.

V. DISCUSSION OF EXPERIMENTAL RESULTS

A. Gd_2CuO_4

Two different magnetic field orientations were measured: parallel to the c axis ($\mathbf{H}_{\parallel z}$) and perpendicular to the c axis ($\mathbf{H}_{\parallel x}$). A magnetic-field-induced electric polarization was measured in both cases perpendicular to the magnetic field corresponding to a projection of the ME-induced polarization $P_x = P_a/\sqrt{2} = \alpha_{ac}H_c/\sqrt{2}$ and $P_z = \alpha_{ca}H_a = \alpha_{ca}H_x/\sqrt{2}$. No induced electric polarization was measured parallel to the magnetic field.

In Fig. 3(a) the field dependence of P_x is shown in magnetic fields $\mathbf{H}_{\parallel z}$ at $T = 5 \text{ K}$ [this component of magnetoelectric susceptibility coincides with χ_{\perp} from Eq. (13)]. The necessary condition for observing the effect was a precedent ME annealing using crossed magnetic and electric fields in accordance with the magnetic symmetry of the system. As is seen from Fig. 3(a) the ME signal disappears, reaching the spin-flip field, and also disappears, raising the temperature above $T_N(\text{Gd})$, as expected from symmetry considerations. The ME signal does not reappear while reentering into the Gd antiferromagnetic phase, suggesting a restoration of the antiferromagnetic domain structure suppressed previously by the annealing procedure.

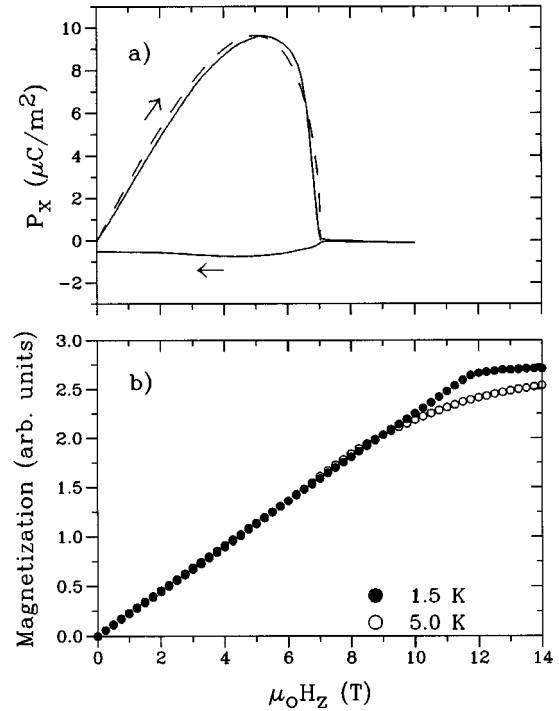


FIG. 3. (a) The electric polarization P_x of Gd_2CuO_4 vs magnetic field $\mathbf{H}_{\parallel z}$ at $T = 5 \text{ K}$ after the ME annealing procedure $E_x = 500 \text{ V/cm}$ and $\mu_0 H_z = 5 \text{ T}$. The dashed line shows the mean-field approximation (see text). (b) For comparison magnetization measurements at 1.5 and 5 K.

In Fig. 3(b) the results of magnetization measurements obtained with the same sample for $\mathbf{H}_{\parallel z}$ at different temperatures are shown for comparison. Whereas the spin-flip transition is clearly observable at 1.5 K, due to the thermal “softening” of the rare-earth sublattices, the spin-flip field is no longer clearly observable at 5 K.¹³ The mean-field approximation $P_x \propto M_z L_x \propto H \sqrt{1 - H^2/H_{\text{sf}}^2}$,⁶ obtained from the last term in Eq. (10), illustrates in Fig. 3(a) the advantage of determining the spin-flip transition H_{sf} from the ME data. The much better resolution of the spin-flip transition in the ME measurements allows a detailed measurement of the $H_{\text{sf}}(T)$ phase diagram. The resulting (H, T) phase diagram as shown in Fig. 4, corrected for the demagnetization factor, has been fitted to a power law $H_{\text{sf}} \propto (T_N - T)^\beta$ for temperatures $T \geq 0.7T_N$ with $\beta = 0.44$. Limiting the range of temperature to more closely to T_N would decrease this critical exponent by 10–15%. The expected critical exponent β from the three-dimensional Heisenberg model equals $\beta = 0.364$ and from the three-dimensional Ising model $\beta = 0.325$, however from the two-dimensional Ising model $\beta = 0.125$. The obtained critical exponent suggests that the ordering of the rare-earth magnetic subsystem is of three-dimensional character, in agreement with experimental results for the temperature dependence of the magnetic susceptibility.⁸

The temperature dependence of the component α_{ac} of the ME susceptibility tensor is shown in Fig. 5. The results have to be taken qualitatively, since each point has been obtained after individual annealing. The expected temperature dependence from Eq. (13) is nevertheless confirmed.

The observation of a ME effect for $P_z(H_x)$ and not for $P_x(H_x)$ and $P_z(H_z)$ (Ref. 6) is in accordance with Eq. (2).

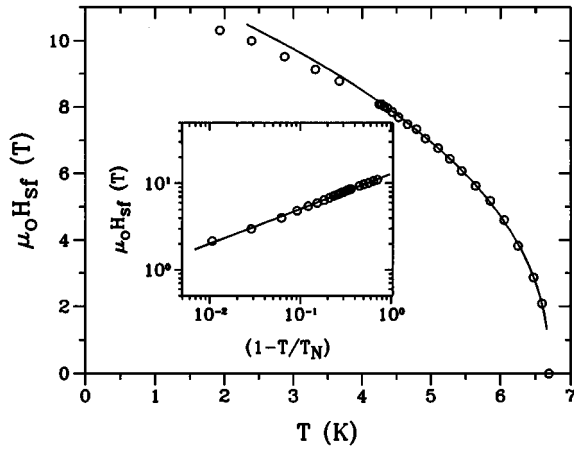


FIG. 4. The spin-flip field H_{sf} of Gd_2CuO_4 as a function of temperature. The solid line is the result of a fit to a power law. The inset shows the corresponding log-log plot.

This implies that the Gd spins are strictly lying in the basal plane as has been proposed from neutron experiments. This is in contradiction with Mössbauer experiments claiming that the direction of the Gd spins is tilted by 45° from the basal plane.¹⁸

B. Sm_2CuO_4

In Fig. 6 the field dependence of P_z is shown for Sm_2CuO_4 in magnetic fields $\mathbf{H}\parallel z$ at different temperatures. The necessary condition for observing the effect was a precedent ME annealing using parallel magnetic and electric fields. For this orientation ($\mathbf{H}\parallel\mathbf{L}$) only the first two terms of Eq. (10) can produce a nonzero electric polarization $\mathbf{P}\parallel z$. In accordance with Eq. (4) the ME signal is a linear function of the magnetic field up to the highest field of 20 T for low temperatures. The temperature dependence of the ME susceptibility α_{cc} is shown in Fig. 7. For higher temperatures approaching $T_N(\text{Sm})$ a critical field H_c is reached where the ME effect disappears while a residual electric polarization remains. This electric polarization is left unchanged for decreasing magnetic fields, suggesting a restoration of the electro-dipole domain structure. The ME effect disappears

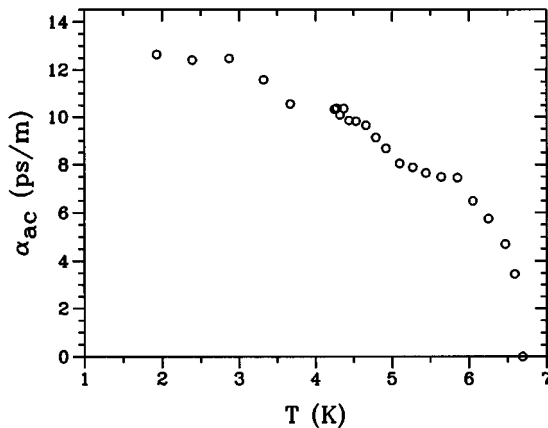


FIG. 5. The temperature dependence of the ME susceptibility α_{cc} of Gd_2CuO_4 .

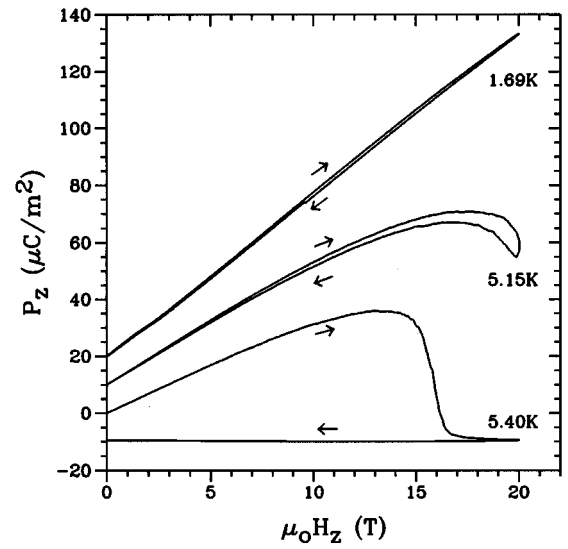


FIG. 6. The electric polarization P_z of Sm_2CuO_4 vs magnetic field $\mathbf{H}\parallel z$ at $T=5$ K after a ME annealing procedure $E_x=500$ V/cm and $\mu_0 H_x=5$ T.

equally for raising the temperature above $T_N(\text{Sm})$. For the observed phase transition at H_c it is not clear whether it is of a spin-flop transition (typical for Heisenberg antiferromagnets) or, most likely, a metamagnetic transition, typical for Ising antiferromagnets.

The observed net ferroelectric moment $\mathbf{P}\parallel z$ at zero magnetic field is incompatible with the magnetic symmetry group $m'm'm'$ that includes anti-inversion. This is to our knowledge the first observation of ferroelectric behavior in this family of compounds.

The observed spin-flip phase transition allows us to construct the $H_c(T)$ phase diagram for Sm_2CuO_4 . The (H, T) phase diagram as shown in Fig. 8, corrected for the demagnetization factor, has been fitted to a power law $H_c \propto (T_N - T)^\beta$ with $\beta \approx 0.5$. This suggests that the inherent ordering of the rare-earth magnetic subsystem is also, like in the case of Gd_2CuO_4 , of three-dimensional character, in agreement with experimental results for the temperature dependence of the magnetic susceptibility.¹² This transition has

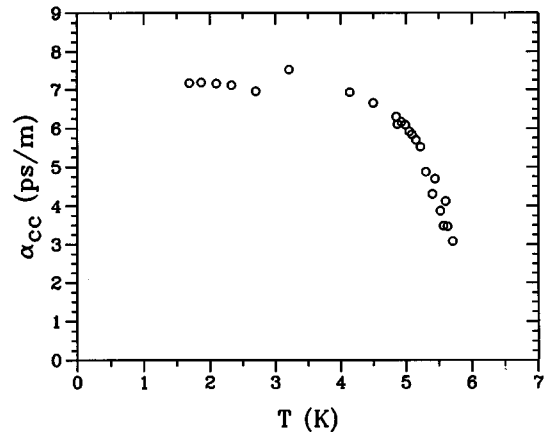


FIG. 7. Temperature dependence of the ME susceptibility α_{cc} of Sm_2CuO_4 .

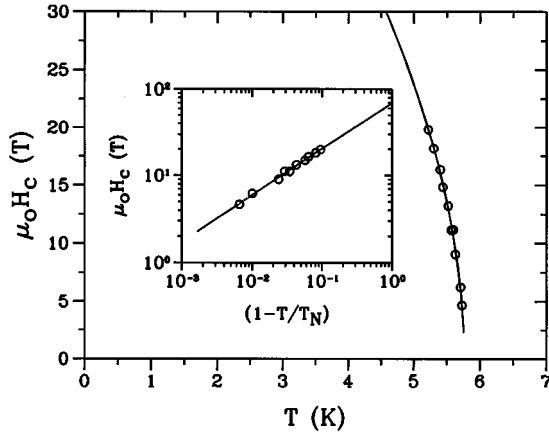


FIG. 8. The critical field H_c of Sm_2CuO_4 as a function of temperature. The solid line is the result of a fit to a power law. The inset shows the corresponding log-log plot.

not been observed before by other experimental techniques, although a shift in T_N (Sm) of 100 mK has been reported in a magnetic field of 11 T by means of specific heat measurements.¹⁹

In Fig. 9 the field dependence of P_x is shown in magnetic fields $\mathbf{H}\parallel x$ at $T=4.2$ K. The necessary condition for observing the effect was a precedent ME annealing using parallel magnetic and electric fields. For this orientation only the first third term of Eq. (10) can produce a nonzero electric polarization $\mathbf{P}\parallel x$. In accordance with Eq. (4) the ME signal becomes a linear function of the magnetic field up to the highest field of 20 T for low temperatures.

C. Nd_2CuO_4

In Fig. 10 the field dependence of P_x is shown in a magnetic field $\mathbf{H}\parallel y$ at 4.2 K. No precedent ME annealing was necessary to observe the effect. The ME effect is quadratic in a magnetic field up to 5 T. At higher fields the character of the dependence $P_x(H_y)$ changes, which might be attributed to a reorientation of the spin structure. For magnetic fields parallel to the x axis no ME effect has been observed.

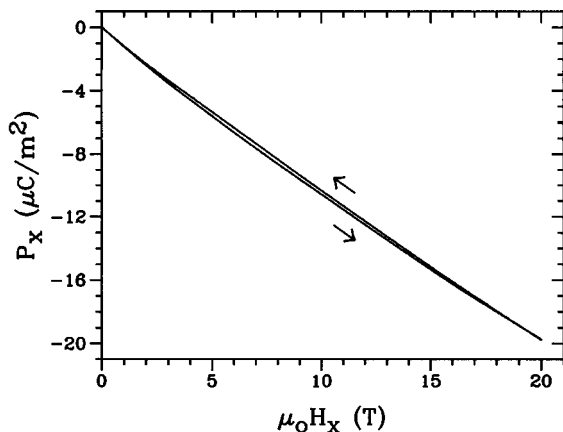


FIG. 9. The electric polarization P_x of Sm_2CuO_4 vs magnetic field $\mathbf{H}\parallel x$ at $T=5$ K after a ME annealing procedure $E_x=500$ V/cm and $\mu_0 H_x=5$ T.

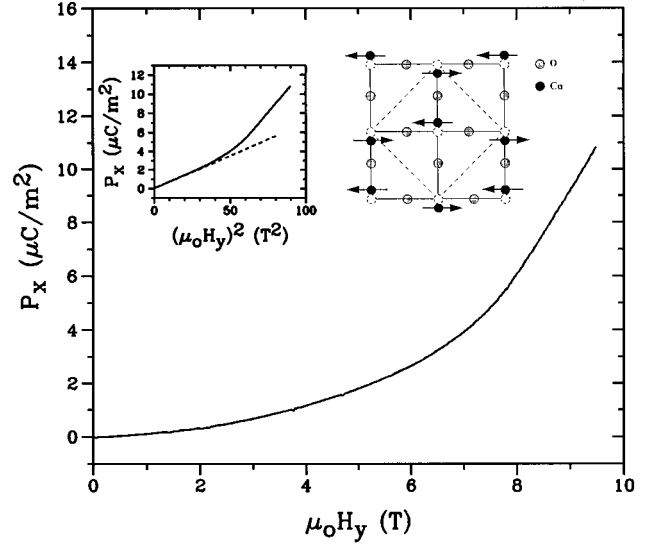


FIG. 10. The electric polarization P_x of Nd_2CuO_4 vs the magnetic field $\mathbf{H}\parallel x$ at $T=4.2$ K. The inset shows the same data vs the magnetic field squared with the dashed line for the zero-field extrapolation. Also the distortion of the CuO_2 is shown schematically.

As we mentioned before, the commonly adopted crystal and magnetic structure of Nd_2CuO_4 supports the existence of space inversion as well as antitranslation. These symmetry operations rule out any sort of ME effect, both linear and nonlinear. Therefore, the very fact of the observation of magnetic-field-induced electric polarization leaves no doubt that the actual crystal and magnetic symmetry of this system is lower than it was thought to be. From the symmetry point of view, the quadratic ME effect is allowed to exist almost in any anisotropic medium without space inversion. The symmetry of such a quadratic-in-field effect is identical to that of the well-known piezoelectric effect, and even the presence of long-range magnetic order is not required. However, one can make sure that any conceivable distortion of the Nd_2CuO_4 tetragonal lattice will never give piezoelectricity. Besides, the structure in the experimentally observed dependence $P_x(H_y)$ (see Fig. 10) suggests a magnetic-field-induced transformation of the antiferromagnetic structure of Nd_2CuO_4 . The observed ME effect is therefore probably associated with a long-range antiferromagnetic order in this compound.

The possible origin for the existence of a magnetic-field-induced electric polarization is the presence of a spontaneous distortion within the CuO_2 planes of the Nd_2CuO_4 crystal structure, which removes space inversion symmetry. The possible distortion patterns which lead to a nonzero ME response have been analyzed in Refs. 22 and 23. The corresponding displacement pattern is presented in Fig. 10. In earlier neutron diffraction experiments^{20,21} the above distortion of the Nd_2CuO_4 crystal structure has been presumably detected. However, the ME effect for this distortion is linear in the magnetic field and not quadratic. To explain this discrepancy, magnetic-field-induced rearrangements of the spin structure could be of importance as well as some special role of the antiferromagnetic domain structure. In view of the possible influence of the domain structure, we note that ME annealing had no influence on the observed effect.

VI. CONCLUSION

In summary, we have investigated in detail the ME effect in the family of compounds with the general formula $R_2\text{CuO}_4$ ($R = \text{rare earth}$) for different orientations of the magnetic field and at different temperatures. For the Gd_2CuO_4 and Sm_2CuO_4 compounds, it has been shown by a symmetry analysis as well as experimentally that the ME effect only exists below the ordering temperature of the rare-earth magnetic subsystem at T_N (Gd,Sm). Although the rare-earth magnetic subsystems of Gd_2CuO_4 and Sm_2CuO_4 are very similar, the compounds belong to different magnetic classes. The ME effect is a powerful tool to distinguish magnetic classes and the experimental results help to clarify the magnetic ground states of Gd_2CuO_4 and Sm_2CuO_4 . For the Nd_2CuO_4 compound, the observed ME effect is directly related to the magnetically ordered Cu system in contrast to the ME effect in the two other compounds.

The observed ME effect in Gd_2CuO_4 is in good agreement with theoretical predictions made in the framework of a symmetry analysis based on the proposed magnetic structure of Gd_2CuO_4 .^{13,24} In this analysis the existence of rare-earth ferromagnetic layers is the crucial feature for the occurrence of the ME effect in Gd_2CuO_4 .

The observed ME effect in Sm_2CuO_4 is also in agreement with theoretical predictions made in the framework of a symmetry analysis based on the proposed magnetic structure of Sm_2CuO_4 .^{15,25} Nevertheless we have revealed a net ferroelectric moment $\mathbf{P}\parallel c$ at zero magnetic field which is only compatible with a lower, polar symmetry group. Most likely, the observed electric polarization has nothing to do with both rare-earth and copper magnetic ordering and is related to some spontaneous distortion of the crystal lattice.

The fact that Sm_2CuO_4 becomes superconducting under doping and exhibits ferroelectric behavior is of particular interest. It has been concluded from investigations of A15 compounds that the appearance of ferroelectricity and superconductivity is mutually exclusive there.²⁶ More recently, investigations of the pyroelectric effect in $\text{YBa}_2\text{Cu}_3\text{O}_{7-\delta}$ have revealed a polar structure in the class of high- T_c superconducting compounds.²⁷

In Nd_2CuO_4 , the ME effect is allowed for a distorted structure of the CuO_2 planes. This gives interesting perspectives for further investigations of the ME effect in this family of compounds since the Cu magnetic subsystem has been proposed to play a role in the superconducting state.

¹Y. Tokura, H. Takagi, and S. Uchida, *Nature* **337**, 345 (1989).

²J.T. Markert, E.A. Early, T. Björnholm, S. Ghamaty, B.W. Lee, J.J. Neumeier, R.D. Price, C.L. Seaman, and M.B. Maple, *Physica C* **158**, 178 (1989).

³H. Takagi, S. Uchida, and Y. Tokura, *Phys. Rev. Lett.* **62**, 1197 (1989).

⁴C.L. Seaman, N.Y. Ayoub, T. Björnholm, E.A. Early, S. Ghamaty, B.W. Lee, J.T. Markert, J.J. Neumeier, P.K. Tsai, and M.B. Maple, *Physica C* **159**, 391 (1989).

⁵S.B. Oseroff, D. Rao, F. Wright, D.C. Vier, S. Schultz, J.D. Thompson, Z. Fisk, S.-W. Cheong, M.F. Hundley, and M. Tovar, *Phys. Rev. B* **41**, 1934 (1990).

⁶H. Wiegmann, A.A. Stepanov, I.M. Vitebsky, A.G.M. Jansen, and P. Wyder, *Phys. Rev. B* **49**, 10 039 (1994).

⁷A.I. Smirnov and I.N. Khlyustikov, *JETP Lett.* **59**, 814 (1994).

⁸J.D. Thompson, S.-W. Cheong, S.E. Brown, Z. Fisk, S.B. Oseroff, M. Tovar, D.C. Vier, and S. Schultz, *Phys. Rev. B* **39**, 6660 (1989).

⁹L.B. Steren, M. Tovar, and S.B. Oseroff, *Phys. Rev. B* **46**, 2874 (1992).

¹⁰I.M. Vitebsky, A.A. Stepanov, T. Chattopadhyay, and P.J. Brown, *Fiz. Nizk. Temp. (Kiev)* **20**, 25 (1994) [*Low Temp. Phys.* **20**, 18 (1994)].

¹¹S. Ghamaty, B.W. Lee, J.T. Markert, E.A. Early, T. Björnholm, C.L. Seaman, and M.B. Maple, *Physica C* **160**, 217 (1989).

¹²M.F. Hundley, J.D. Thompson, S.-W. Cheong, Z. Fisk, and S.B. Oseroff, *Physica C* **158**, 102 (1989).

¹³T. Chattopadhyay, P.J. Brown, A.A. Stepanov, P. Wyder, J.

Voiron, A.I. Zvyagin, S.N. Barilo, D.I. Zhigunov, and I. Zobkalo, *Phys. Rev. B* **44**, 9486 (1991).

¹⁴J.W. Lynn, I.W. Sumarlin, S. Skanthakumar, W.-H. Li, R.N. Shelton, J.L. Peng, Z. Fisk, and S.-W. Cheong, *Phys. Rev. B* **41**, 2569 (1990).

¹⁵I.W. Sumarlin, S. Skanthakumar, J.W. Lynn, J.L. Peng, Z.Y. Li, W. Jiang, and R.L. Greene, *Phys. Rev. Lett.* **68**, 2228 (1992).

¹⁶Y. Dalichaouch, B.W. Lee, C.L. Seaman, J.T. Markert, and M.B. Maple, *Phys. Rev. Lett.* **64**, 599 (1990).

¹⁷We are grateful to S.N. Barilo and D.I. Zhigunov for supplying us with samples of Gd_2CuO_4 , Sm_2CuO_4 , and Nd_2CuO_4 .

¹⁸P. Adelmann, R. Ahrens, G. Czjzek, G. Roth, H. Schmidt, and C. Steinleitner, *Phys. Rev. B* **46**, 3619 (1992).

¹⁹T. Holubar, G. Schaudy, N. Pillmayr, G. Hilscher, M. Divis, and V. Nekvasil, *J. Magn. Magn. Mater.* **104–107**, 479 (1992).

²⁰S. Skanthakumar, H. Zang, T.W. Clinton, W.-H. Li, J.W. Lynn, Z. Fisk, and S.-W. Cheong, *Physica C* **160**, 124 (1989).

²¹J.M. Rosseinsky and K. Prassides, *Physica C* **162–164**, 522 (1989).

²²I.M. Vitebsky, N.M. Lavrinenko, and V.L. Sobolev, *J. Magn. Magn. Mater.* **97**, 263 (1991).

²³V. Blinkin *et al.*, *Sov. Phys. JETP* **71**, 1179 (1990).

²⁴T. Chattopadhyay, P.J. Brown, B. Roessli, A.A. Stepanov, S.N. Barilo, and D.I. Zhigunov, *Phys. Rev. B* **46**, 5731 (1992).

²⁵S. Skanthakumar, J.W. Lynn, J.L. Peng, and Z.Y. Li, *J. Appl. Phys.* **69**, 4866 (1991).

²⁶L.R. Testardi, *Rev. Mod. Phys.* **47**, 637 (1975).

²⁷D. Mihailović, I. Poberaj, and A. Mertelj, *Phys. Rev. B* **48**, 16 634 (1993).